

PCCP

Accepted Manuscript

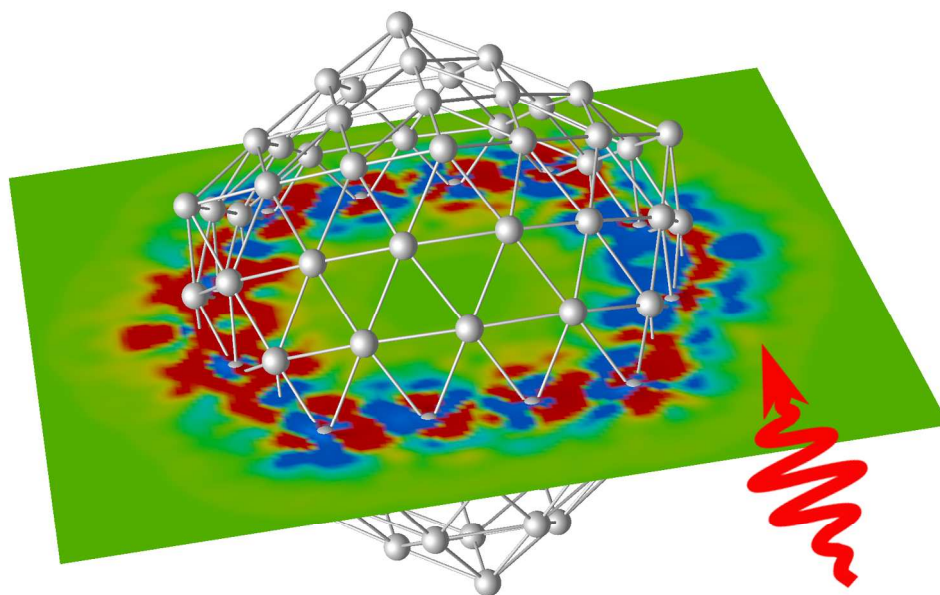


This is an *Accepted Manuscript*, which has been through the Royal Society of Chemistry peer review process and has been accepted for publication.

Accepted Manuscripts are published online shortly after acceptance, before technical editing, formatting and proof reading. Using this free service, authors can make their results available to the community, in citable form, before we publish the edited article. We will replace this *Accepted Manuscript* with the edited and formatted *Advance Article* as soon as it is available.

You can find more information about *Accepted Manuscripts* in the [Information for Authors](#).

Please note that technical editing may introduce minor changes to the text and/or graphics, which may alter content. The journal's standard [Terms & Conditions](#) and the [Ethical guidelines](#) still apply. In no event shall the Royal Society of Chemistry be held responsible for any errors or omissions in this *Accepted Manuscript* or any consequences arising from the use of any information it contains.



Absorption spectra of hollow Ag and Au clusters are compared to compact clusters; compression has little influence on optical spectra

Optical Response of Quantum-Sized Ag and Au Clusters — Cage vs. Compact Structures and the Remarkable Insensitivity to Compression[†]

Hans-Christian Weissker^{a,b}, Robert L. Whetten^{*c}, and Xóchitl López-Lozano^{*c}

Quantum-sized silver and gold clusters show very different spectral characteristics. While silver exhibits a strong localized surface-plasmon resonance (LSPR) band down to very small sizes, the resonance is broadened beyond recognition in Au clusters below about 2 nm. In the present work, we study icosahedral hollow-shell structures, or cages, of about 1.8 nm diameter in comparison with compact clusters and show that the qualitative difference between Ag and Au remains but is reduced, as a significant increase of absorption is found for the Au cage structures. The silver shell Ag_{92} exhibits a resonance that is red-shifted compared to the compact Ag_{147} , coinciding with the general result found in much larger shells that are amenable to the classical description by Mie theory. However, the electronic structure in particular of the d band is strongly changed. The spectrum of the empty Ag shell is remarkably similar to the spectrum of the respective $\text{Ag}_{92}\text{Au}_{55}$ core-shell structure. Inspection of the time-dependent electronic density does not explain this similarity. However, it shows that the overall classical picture of a collective charge oscillation remains valid, although clearly with modifications. We further show a remarkable insensitivity of the absorption spectra of both Ag and Au clusters to even rather extreme values of compression or dilatation.

The outstanding optical properties of noble-metal clusters and nanoparticles (NPs) are the basis of a large number of interesting applications that make use of the localized surface-plasmon resonances (LSPR) that dominate the clusters' optical response in the visible and the ultraviolet spectral regions. Applications include surface-enhanced Raman spectroscopy (SERS),¹ biomolecule sensing,² labeling of biomolecules,³

cancer therapy,⁴ the plasmonic absorption enhancement in solar cells,⁵ and nanophotonics.⁵

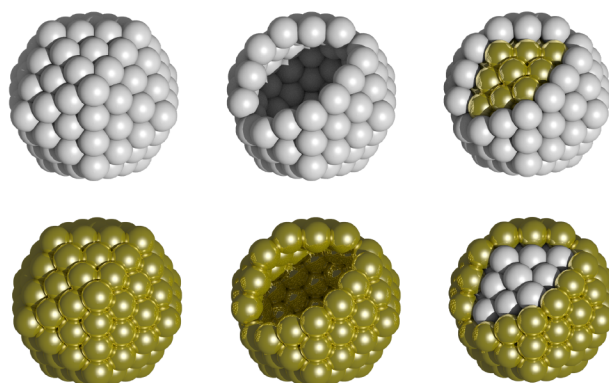


Fig. 1 The six cluster structures used in the present work are derived from the 3-shell Mackay icosahedral structure comprising 147 sites, distributed in concentric shells of 12, 42, and 92 sites about a unique central site. The 92-atom empty shell (middle panels) is the outermost shell of the full 147-atom cluster (left panels). The bimetallic core-shell cluster (right panels) consists of a 55-atom core and the 92-atom outer shell. In the figure, some atoms of the shell have been removed to make the nature of the structures visible. The figure shows the pure compact icosahedron Ag_{147} , the pure shell Ag_{92} , and the $\text{Au}_{55}\text{Ag}_{92}$ core shell cluster (upper row). We likewise study the converse cases Au_{147} , Au_{92} , and $\text{Ag}_{55}\text{Au}_{92}$ (lower row).

Applications require tunability of the LSPR.⁶ The resonance is both material and geometry dependent. Nanoshells, as opposed to compact clusters, are particularly interesting because their optical cross sections are comparable to or even higher than those of compact clusters.⁷ However, the resonance energy can be strongly decreased by either increasing the shell radius or by decreasing the shell thickness. The optical resonance can be tuned to lie favorably in the near-IR region useful for *in vivo* imaging and therapeutical applications.⁷ For instance, it lies at 892 nm for a silica-gold nanoshell with core radius of 60 nm and 10 nm shell thickness.⁷ At this energy, tissue transmissivity is highest⁸ and the energy is well separated from the hemoglobin visible absorption around 500-600 nm.⁹ The core medium has likewise an

[†] Electronic Supplementary Information (ESI) available: We show the spectra of the shell and core-shell clusters scaled for better visibility on like scales between Ag and Au, as well as to show the absorption per atom. Moreover, we show the time-dependent dipole moment and the points in time when the snapshots of Fig. 4 were taken. See DOI: 10.1039/b000000x/

^a Aix Marseille University, CNRS, CINaM UMR 7325, 13288, Marseille, France

^b European Theoretical Spectroscopy Facility

^c Department of Physics & Astronomy, The University of Texas at San Antonio, One UTSA circle, 78249-0697 San Antonio, TX, USA; Xochitl.LopezLozano@utsa.edu

influence on the LSPR and provides a means of tuning the resonance.¹⁰

The bulk of literature concerns shells larger than a few tens of nm. Most calculations of the optical properties have been done using classical theory (Mie theory;^{7,10,11} discrete dipole approximation (DDA)^{7,12}). The general results, in agreement with the experimental findings, are a red shift both with decreasing shell thickness and, for constant thickness, with increasing shell radius.¹¹ However, the classical description relies on the assumption that the dielectric function of the material remains valid for the nanostructures.

While the classical description does well for these “large” nanoparticles, it does not describe the spill-out of the conduction electrons nor the reduced screening by the *d* electrons at a thin surface layer,¹³ and even less the quantum-size effects that can change position, width, and shape of the *d* band. These quantum effects become increasingly important for smaller sizes. In very small clusters, the bands split into discrete levels; at a certain point, the concept of the dielectric function becomes questionable altogether. The optical spectra reflect this transition. We have recently shown that the widely studied and applied Au₁₄₄(SR)₆₀ cluster compound—a cluster of an intermediate size that has been thought large enough to produce *necessarily* smooth spectra—is replete with individual peaks that reflect the quantum nature of the system.¹⁴ It goes without saying that these spectra are not amenable to the classical description. Moreover, the response of pure clusters in this size range has been shown to depend on the precise atomic arrangement.¹⁵ Clearly, these effects require an atomistic quantum-physical approach for a correct description of the optical spectra of “quantum-sized clusters.” Time-dependent density-functional theory (TDDFT) provides the basis for the proper treatment of the excitations, initially based on jellium-type background models^{13,17} that cannot, however, describe the inhomogeneity at the atomistic level, and, subsequently, based on pseudopotentials or localized orbitals.

Atomistic TDDFT calculations of optical spectra have been done for tetrahedral silver structures of up to 120 atoms by Aikens *et al.*,¹⁸ for other gold and silver structures of comparable numbers of atoms,^{19,20} for Au and Ag chains,²¹ and for nanorods^{22,23} and helical chains²⁴ as well as for pure^{15,25} and bimetallic^{26,27} high-symmetry clusters of up to 147 atoms. Monolayer-protected clusters have likewise been studied, mostly with thiolate ligands^{28–30} Very recently, a calculation of Au₃₁₄(SH)₉₆ has been reported.³¹ The influence of different approximations of the electronic exchange and correlation have been systematically studied recently for silver clusters.³² Mostly done using the transition-based Casida approach,^{33,34} calculations are heavy because a large number of Kohn-Sham transitions needs to be taken into account to describe the excitations well. In the present work, we use the time-evolution approach.³⁵ The advantage of the method is that one does not

need to calculate a large number of empty states; the calculations are, therefore, numerically much less heavy. Naturally, the necessarily finite propagation time introduces a broadening of the transitions that make up the spectra. The disadvantage of the method is that the information about the origin of individual features in the spectra is not directly obtained.

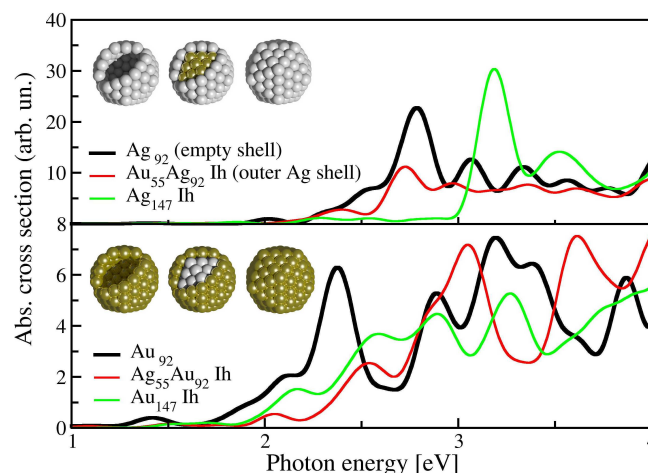


Fig. 2 Upper panel: absorption spectra of the silver-based clusters: the shell Ag₉₂, the core-shell structure Au₅₅Ag₉₂ Ih (outer Ag shell), and the compact Ag₁₄₇ Ih. Lower panel: the same for the respective gold-based structures: the shell Au₉₂, the core-shell structure Ag₅₅Au₉₂ Ih, and the compact Au₁₄₇ Ih. Note the different scales; the absorption of the Ag-based clusters is significantly stronger throughout. A comparison of the spectra on the same scale is given in Fig. S 1 of the SI.

Unlike the larger nanoparticles, quantum-sized globular gold and silver clusters, i.e., those where the quantum effects are important, show very different optical properties. In Ag NPs, the LSPR is observed down to very small sizes (fewer than 20 atoms).³⁶ By contrast, small Au clusters below about 2 nm do not show this resonance.^{15,37–40} However, the precise conditions for the emergence of the LSPR in gold clusters are not yet well understood. On the one hand, the LSPR seems to develop between sizes of 100 and 300 atoms.^{31,41,42} On the other hand, the role of composition and environment is still not entirely clear. Recently, it was shown by Dass and coworkers that the incorporation of Cu into the Au₁₄₄ cluster apparently leads to a plasmon-like resonance.⁴³ The interesting conclusion is that the combination of two materials that do not show a resonance at this size is apparently becoming “plasmonic.”

The reason for the qualitatively different behavior of quantum-sized globular Au and Ag clusters is the different energetic position of the respective *d* electrons. In Ag, the filled *d* shell lies at about 4 eV below the Fermi surface, which means that the energy of the LSPR is well below the onset of “interband transitions” from the *d* band into unoccupied states above

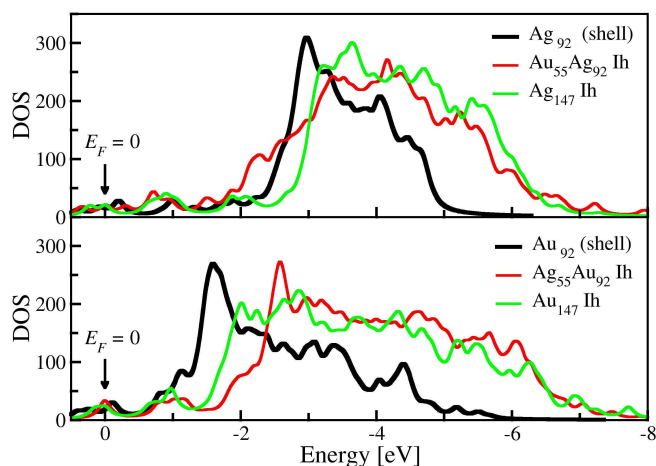


Fig. 3 Electronic density of occupied states. The energies are the Kohn-Sham energies of the ground-state DFT calculation. The zero of the energy axis is the Fermi energy. A broadening of 0.1 eV has been applied.

the Fermi energy. The LSPR is, therefore, largely decoupled from these transitions. By contrast, the onset of the 5d band of compact Au clusters lies at about 2 eV, with little variation with size.⁴⁴ The LSPR, found for bigger globular Au clusters between 2.3 and 2.6 eV,¹³ is therefore strongly coupled to the interband transitions which damp and broaden the resonance beyond recognition in small clusters. Moreover, it has been shown that the optical spectra of, for instance, Cu shells are decisively influenced by the interband transitions, exhibiting a double-peak feature in the spectrum.⁴⁵

Due to the importance of the interband transitions from the *d* band, any parameter that changes the electronic *d* band is likely to influence the optical properties of, in particular, Au clusters strongly. Interestingly, when the aspect ratio of the NP is changed so as to lower the energy of the LSPR, the resonance can be decoupled from the interband transitions and appears strongly in nanorods of sizes of about 100 atoms, i.e., at a size at which spherical clusters do not show the resonance.^{22,23} Due to the geometry-governed red-shift of the LSPR, one could imagine that a similar effect could be found in the quantum-sized gold shells.

We have shown in earlier work on Ag-Au nanoalloys that the outermost shell of the quantum-sized core-shell clusters is decisive for the character of the response, determining, in particular, if the cluster becomes “silver-like,” i.e., plasmonic, or “gold-like,” i.e., without a clear LSPR.^{15,16} The preponderance of the outermost shell (and the implied lesser importance of the inner core) raises the question as to what the response would be of the outermost shell alone. Clearly, a strong change of the *d* band is expected due to the change of the average coordination of the gold atoms.

Gold, in particular, is known to produce cage structures.⁴⁶ For instance, a 72-atom fullerene-like icosahedral gold shell has been shown theoretically to possess a high thermodynamic stability and a rather large gap.⁴⁷ The Au cages are generally rather complex structures. The resulting spectra are molecular-like and not easily interpretable, in particular because the precise atomic structure influences the spectra strongly for these sizes.¹⁵ For the same reason, they are not easily compared to the spectra of compact clusters. Consequently, in order to keep direct comparability with compact structures, we chose to study the outermost shells of the icosahedral Au₁₄₇ and Ag₁₄₇ clusters as model structures, viz., Au₉₂ and Ag₉₂. This allows a direct comparison with both the compact pure and core-shell structures investigated before.¹⁶ The lower coordination of the shell atoms compared to a compact cluster or the bulk material will strongly influence the filled *d* shell and, therefore, potentially the absorption spectra.

Apart from the change of coordination, a second factor that potentially changes the position and the width of the *d* band are the interatomic distances within the cluster. This raises the question if compression or dilatation of the structure, as they might arise in different situations, will influence the optical properties decisively. From the experimental point of view, this is important because different surroundings and ligands may induce such changes. From the point of view of theoretical studies, this is likewise of interest because the most widely employed functionals of DFT show systematic errors in lattice constants and interatomic distances: the local-density approximation (LDA) usually underestimates bond lengths by about 2%, while the generalized gradient approximation (GGA; also used in the present study) leads to a slight overestimation. It is, consequently, important to know if these differences will decisively change calculated spectra or not.

In the present work, we study the difference between the optical properties of hollow-shell structures and compact pure and core-shell clusters. Moreover, we investigate the influence of compression and dilatation on the optical spectra. Comparison with the density of occupied states yields partial interpretation of the spectra. Moreover, the time-dependent electronic density is analyzed and compared with the classical picture of the LSPR as a collective charge oscillation.

1 Model structures and computational details

The icosahedral 147-atom cluster is one of a series of “magic” sizes of particular stability.⁴⁸ The clusters have a shell structure centered around one atom. The outermost shell contains 92 atoms. Furthermore, we study the bimetallic Au₅₅Ag₉₂ and, conversely, Ag₅₅Au₉₂ where the core of 55 atoms is surrounded by the 92-atom outermost shell. The relaxation of both the compact pure 147-atom clusters and of the core-shell structures was done using the VASP code^{49,50} and the PW91

gradient-corrected functional.⁵¹ To obtain the shell model structure, we use the geometry of the relaxed 147-atom Ag and Au clusters and take the outermost shell without further relaxation. The structures are depicted in Fig. 1. All the clusters investigated in the present study have the full icosahedral symmetry I_h . Their response is isotropic; the response was calculated for one direction. In order to model compression or dilatation of the pure clusters, we take the 147-atom compact icosahedra and modify the interatomic distances by a common factor.

Absorption spectra are calculated using time-dependent density-functional theory as implemented in the real-space code `octopus`.^{52,53} After a ground-state calculation, spectra are calculated using the time-evolution formalism.³⁵ Norm-conserving Troullier-Martins pseudopotentials have been used which include the d electrons in the valence, that is, with 11 valence electrons for each atom. The gradient-corrected PBE exchange-correlation potential has been used. A comparison of different functionals is shown in the supplementary material of reference Refs. 23. The real-space grid spacing was set to 0.18 Å for the silver and mixed clusters and to 0.20 Å for gold, the radius of the spheres centered around each atom which make up the calculation domain to 5 Å. The evolution time was 25 fs, corresponding to a broadening of the spectra of about 0.15 eV. The time step for the propagation was 1.97×10^{-3} fs for the pure Au cluster and 1.58×10^{-3} fs for the clusters containing Ag.

We have successfully used the same numerical set-up to calculate absorption spectra of pure¹⁵ and bimetallic¹⁶ clusters, of nanorods of up to 263 gold atoms,²³ and of the $\text{Au}_{144}(\text{SR})_{60}$ thiolate gold cluster compound.¹⁴ The spectra obtained with the time-evolution method are equivalent to spectra obtained in Casida's approach. Tests for a bare Au_{20} tetrahedron and a thiolated cluster are shown in the supplementary material of Refs. 23 and 14.

Spin-orbit coupling is neglected in our calculations. The spin-orbit coupling can split and somewhat shift transitions that without it are degenerate. Calculations explicitly including the spin-orbit interaction have been reported for very small Au clusters.⁵⁴ For small monoatomic chains, the splittings are very large; for more compact clusters, the effect tends to be quenched. In the case of, e.g., the Au_{20} tetrahedron, the changes to the spectra are not enormous but neither negligible. Moreover, Stener *et al.* have studied WAu_{12} and MoAu_{12} clusters,⁵⁵ showing that the inclusion of spin-orbit coupling is important in the low-energy range of these small clusters where single transitions dominate. Finally, for semiconductors, a calculation including spin-orbit coupling for a 41-atom hydrogenated Ge cluster has shown a significant splitting of the lowest absorption peak.⁵⁶ In general, while individual peaks can be influenced rather strongly, the overall form of the spectra will only be changed slightly. Therefore, a change in the char-

acter or a drastic change of the spectra presented in the present work is not expected.

2 Results

2.1 Shell structures vs. compact clusters

The optical absorption spectra of the shell structures are shown in Fig. 2 and compared with the spectra of the compact clusters and the core-shell structures.

The most obvious finding is that the qualitative difference Au vs. Ag remains unchanged, although it is reduced because for the Au shell, there is a rather strong increase of the absorption at about 3.3 eV compared to the compact Au_{147} . Nonetheless, the absorption remains much weaker than that of the Ag structures with its rather clear LSPR. (Note the different scales in the figure. A comparison on the same scale is given in the SI, Fig. S 1.)

Second, it is notable that the resonance of the Ag cluster persists, with an intensity comparable to that of the compact Ag_{147} . It is, however, red-shifted by 0.4 eV. Comparison with the density of states in Fig. 3 shows that the resonance remains well below the onset of possible interband transitions from the d band. The shape of the typical d band is clearly visible in the DOS. The band is narrower compared to that of the compact cluster, which is the standard behavior expected due to the lower average coordination of the atoms. Moreover, the onset of the band is shifted upwards, towards the Fermi energy, by about 0.3 eV. This can be correlated with the red-shift of the secondary structures (at about 3.6 eV in the compact cluster) which have been concluded to stem from interband transitions.¹⁶ Finally, the DOS of the core-shell cluster $\text{Au}_{55}\text{Ag}_{92}$ is intermediate between the DOS of the Au and the Ag clusters. In view of the importance of the interband transitions from the d band for the dielectric function, these changes confirm that reliance on the bulk electronic structure and dielectric function may introduce enormous errors; the classical description of the LSPR cannot be expected to remain valid for the quantum-sized clusters. Nonetheless, the red-shift of the resonance is coherent with the redshift found in much larger structures and by classical Mie theory.¹¹

It is somewhat surprising, however, to compare the absorption spectrum of the shell with the spectrum of the core-shell structure where a 55-atom Au core is surrounded by the 92-atom silver shell.¹⁶ Also in this case, a resonance is present, at an energy almost exactly equal to that of the shell; the resonance peak as well as the secondary structures at higher energies are only a bit more broadened than in the case of the shell. The absorption per atom is stronger in the case of the shell (cf., Fig. S 2 of the SI). However, one cannot generalize and conclude from this similarity that the nature of the interior of the shell does not matter. Previous work has shown

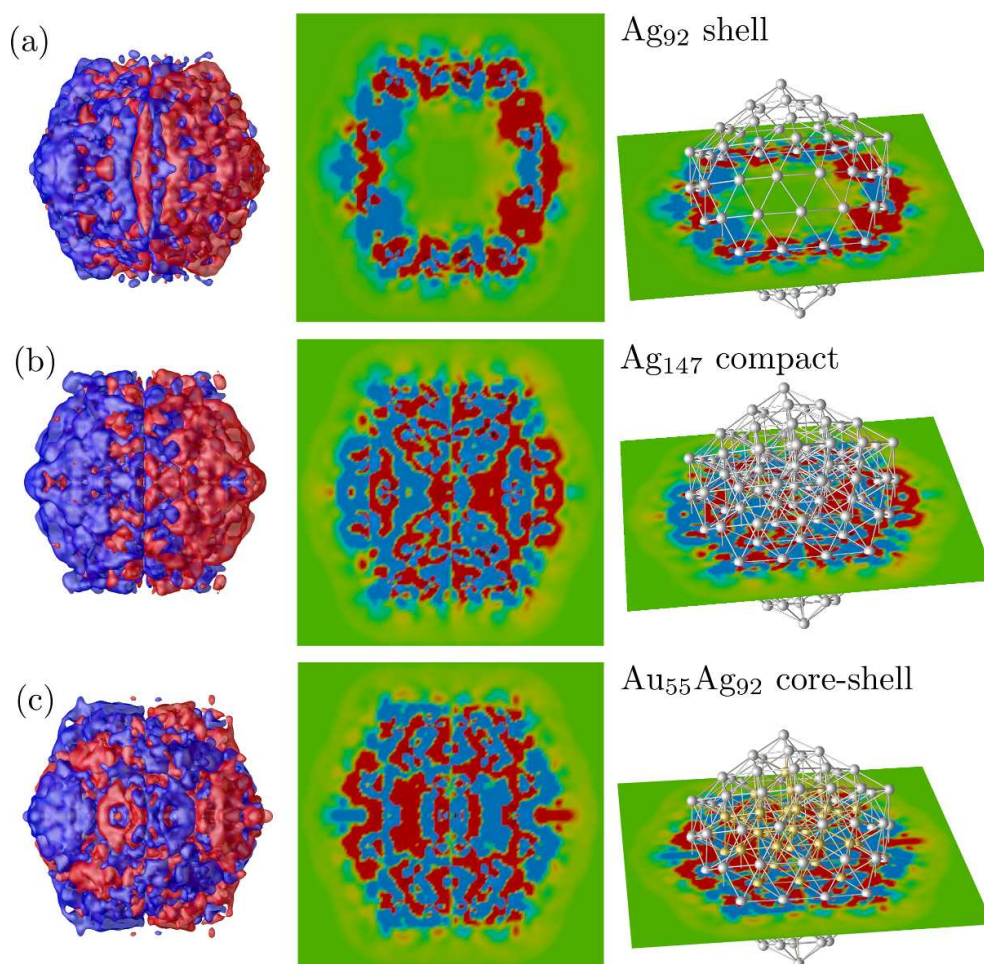


Fig. 4 Snapshots of the time-dependent electronic density for the Ag shell, the compact silver cluster, and the core-shell cluster with one outer shell of Ag atoms and a gold core. Shown is the difference of the density with respect to the ground-state density: left panels: isosurfaces at 2×10^{-5} (red is positive, blue negative). Center panels: cross section through the center of the clusters; red = 2×10^{-5} , blue = -2×10^{-5} . The right-hand side shows the position of the cross section with respect to the cluster geometry. The points in time when the respective snapshots were taken during the time evolution are indicated in Fig. S 3 of the SI.

large differences for core-shell clusters with outer Ag shell and cores of Au or Cu.¹⁵ Experimental work on larger shells likewise shows that the response depends on the core that “fills” the shell.¹⁰

As the spectra of the silver shell and the AuAg core-shell structure are similar, one could expect this similarity reflected in the dynamics of the electronic density. The classical picture of the LSPR is a collective oscillation of the sp conduction electrons. The external field of, say, a laser will set the oscillation in motion; if the collective oscillation is dominant, it will remain stable over many periods. In the case of the time evolution method that we employ to calculate the absorption spectra, all wave functions have a velocity imposed at $t = 0$. After this perturbation, the electronic states and, therefore, the electronic density, evolve freely.³⁵ The resulting total dipole moment as a function of time is given in Fig. S 3 of the SI. In order to picture the spatial behavior of the density, we chose an instant of maximal dipole moment after the end of the 25 fs time span of the calculation that obtains the optical spectra. The snapshots are indicated by the crosses in Fig. S 3 of the SI. The spatial distribution of the density change (or, more precisely, the difference with respect to the ground-state density) is shown in Fig. 4 for the silver shell Ag₉₂, the compact silver cluster Ag₁₄₇, and the core-shell cluster Au₅₅Ag₉₂. In each of these cases we show the isosurfaces, a slice through the middle of the cluster, and the same slice in relation with the geometry. It is evident from the isosurfaces that the overall classical picture of a collective charge oscillation is at least approximately valid for all the structures, although the core-shell structure shows more details overlaid on the overall polarization. Looking at the slice through the Ag₉₂ shell, one sees that while there is the overall polarization, a finer pattern is likewise visible, in particular opposed to the outer polarization on the faces perpendicular to the direction of the excitation. This suggests that the shell is not only polarized as a whole on the outside, but that there is a certain opposite polarization at the two sides of the single layer of atoms perpendicular to the direction of the excitation.

In the case of the compact Ag₁₄₇, the overall polarization is very clear on the outside. However, even here the cross section shows that inside the cluster, there is a fine pattern of local polarization that in part opposes the average polarization. Two reasons for this are imaginable: (i) different modes of collective oscillations of the sp electrons might be involved, and, (ii) the polarizable d electrons show here the opposite polarization to the overall displacement of the electron cloud, thereby creating the screening effect that is decisive for the energy of the LSPR.¹³ We likewise consider instants of zero overall dipole moment as indicated in Fig. S3 of the Supplementary Information. The corresponding snapshots are shown in Fig. S4 of the Supplementary Information. We observe that at these times, a finer pattern of minor modes is present. These

“fluctuations” deviate from the overall intuitive picture of one coherent charge oscillation mode. A serious future study carrying out a detailed analysis of the spatial patterns of the time-dependent electronic density could produce important insights into the physics of the clusters.

Finally, the core-shell cluster with the Au core shows a pattern of the interior polarization similar to that of the compact Ag₁₄₇. The fact that the Au 5d electrons are closer to the Fermi energy makes them more polarizable, thereby interfering more strongly with the collective oscillation of the d electrons. In the core-shell structure, this leads to a stronger perturbation of the overall polar picture of the average polarization compared to the pure-Ag case. This analysis does not, however, explain the strong similarity of the spectra of the hollow-shell and the core-shell structure. The spatial patterns of the time-dependent density are clearly very different because of the empty interior of the hollow-shell where both the density and, consequently, the density differences are approximately zero.

The absorption spectra of the Au-based clusters are shown in the lower panel of Fig. 2. As already mentioned, the basic character of the gold clusters remains qualitatively unchanged for the shell structure. However, there is a clear increase of absorption in the visible range, in particular with the peak at about 2.35 eV. The effect is similar to the intensity increase of larger shells.¹¹ Nonetheless, this peak is of an intensity comparable with that of the structures higher in energy and, in particular, much lower than the absorption in the respective silver clusters, cf., Fig. S 1 of the SI. One could argue that the strong increase of the peak at 2.35 eV corresponds to the incipient emergence of the LSPR because of the geometry-induced red-shift and the resulting beginning decoupling from the interband transitions, similar to the case of Au nanorods.²³ In addition, the lowest peak in the gold-shell spectrum has a shape very similar to that of the peak of the Ag shell. However, the present analysis does not allow for so strong a conclusion.

Comparison of the density of states for the gold-based clusters shows similar effects as in the silver clusters: the hollow-shell's DOS shows a narrower 5d band and its onset is shifted upwards, closer to the Fermi energy. In addition, the onset is slightly steeper. In any case, possible interband transitions into states above the Fermi energy cover the full range of the spectra in the visible. This remains true even though the DOS shown here refers to energies of the Kohn-Sham states from static DFT. The difference between Ag and Au is clearly reflected here.

2.2 The influence of compression

The second parameter that has a bearing on the energy and shape of the d band is compression or dilatation or, in other words, the influence of changes of the interatomic distances.

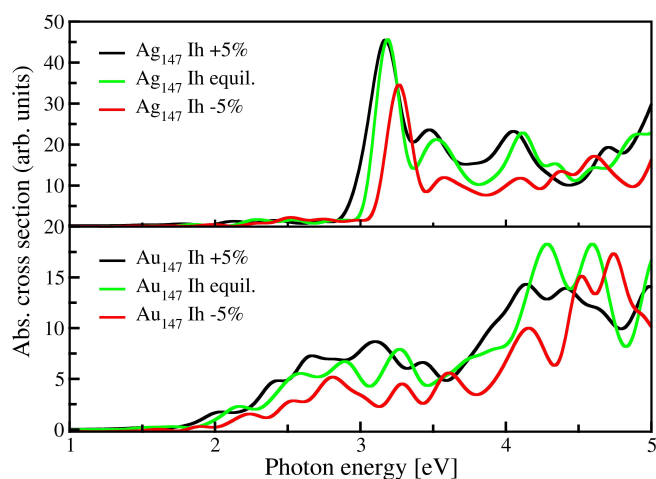


Fig. 5 Absorption spectra for Ag (upper panel) and Au (lower panel) compact clusters for different values of compression or dilatation, respectively. “Equilibrium” denotes the relaxed cluster, while -5% and +5% denote the respective change of the interatomic distances.

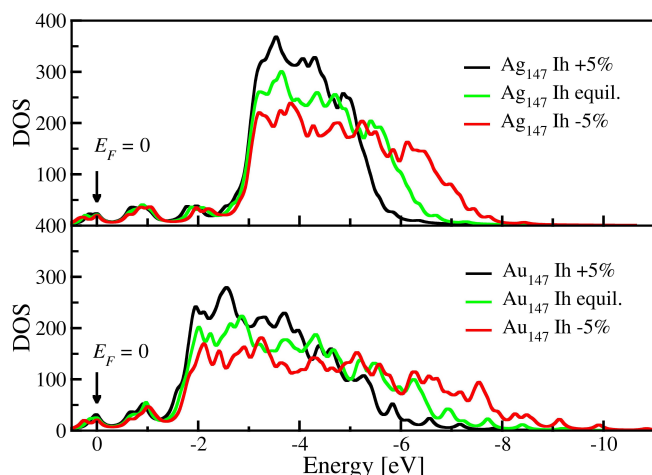


Fig. 6 Density of states of the Ag-based (upper panel) and Au-based (lower panel) for different values of compression or dilatation, respectively. “Equilibrium” denotes the relaxed cluster, while -5% and +5% denote the respective change of the interatomic distances. The energies are the Kohn-Sham energies of the ground-state DFT calculation. The zero of the energy axis is the Fermi energy. A broadening of 0.1 eV has been applied.

The spectra of both the Ag-based and the Au-based compact 147-atom clusters are shown in Fig. 5. We show the spectra of the equilibrium structures as well as compressed by 5% and dilated by the same amount. In view of the situations found in experiment, these values reflect extreme compression and dilatation. Nonetheless, the spectra show a remarkable insensitivity to these extreme structural changes. Also here, the qualitative difference silver-like vs. gold-like remains entirely unchanged. Moreover, the LSPR in Ag changes very little: the shift is almost zero upon dilatation, and less than 0.1 eV upon compression. For the gold clusters, the changes are likewise small and by no means qualitative. In general, this result shows a surprising insensitivity of the metal-cluster-specific optical properties to strong compression.

We can again correlate these results with the DOS of the occupied states. With decreasing interatomic distances, the *d* band becomes broader, as expected. However, there is only a very small shift of the onset of the *d* band with respect to the Fermi energy. For the silver clusters, this shift (of the order of 0.1 eV between +5% and -5%) corresponds exactly to the shift of the secondary structures at about 3.5 eV in the spectra. This is another corroboration that these wide peaks are due to interband transitions from the *d* band.

3 Conclusions

We have studied the general tendencies that distinguish quantum-sized hollow-shell or cage structures from compact clusters. In order to do so, we have considered the outermost shell of the well-studied 147-atom icosahedral cluster, viz., the 92-atom cage structure, in comparison with the compact clusters. Changes in the electronic structure, demonstrated here by the changes in the DOS in particular of the filled *d* band, show that a classical description relying on a bulk dielectric function cannot be used uncritically. In the quantum-sized globular clusters, the qualitative difference between Ag and Au, well known for compact clusters, remains basically unchanged for the shells: the silver-based clusters show a strong localized surface-plasmon resonance, while the absorption of the gold-based clusters is much weaker. There is, however, a clear *increase* of the absorption *per atom* for the cage structures compared to the compact clusters. It is imaginable that larger shell radii will have lower resonance energies, which could decouple the LSPR from the interband transitions sooner than in the compact clusters, similar to the situation in gold nanorods.^{22,23}

The silver shell Ag₉₂ exhibits a resonance that is red-shifted compared to the compact Ag₁₄₇ which is consistent with the classical result for larger shells. Somewhat surprisingly, the spectrum of the hollow-shell is rather similar to the spectrum of the Au₅₅Ag₉₂ core-shell structure. However, in view of previous work, one cannot generalize and conclude that the interior of the shell does not matter. Analysis of the time evolution

of the electronic density shows that the LSPR corresponds to the classical picture of a collective charge oscillation, although the oscillation is by no means homogeneous over the volume of the clusters. However, inspection of the time-dependent electronic density does not explain the similarity of the hollow silver shell Ag₉₂ and the Au₅₅Ag₉₂ core-shell cluster.

The study of compression or dilatation of the compact clusters reveals a surprising insensitivity of the spectra to this parameter. The LSPR of the silver clusters undergoes only a tiny shift, as do the interband-related features of the spectra. The *d* band narrows systematically with increasing interatomic distances. However, the shift of the bands with respect to the Fermi energy remains small, although systematically visible. The qualitative difference between Au and Ag remains unchanged. The changes of the gold-cluster spectra are likewise small.

4 Acknowledgments

The artwork (Fig. 1) was prepared by Clemens Barth (CINaM-Marseille) with Blender (<http://www.blender.org>) and the Atomic Blender addons. XLL acknowledges funding from NSF-DMR-1103730 and NSF-PREM DMR-0934218. The work received computational support from Computational System Biology Core, funded by the National Institute on Minority Health and Health Disparities (G12MD007591) from the National Institutes of Health, as well as the Texas Advanced Computing Center (TACC) at The University of Texas at Austin and HPC resources from GENCI-IDRIS (Grant 2013-096829). Moreover, we acknowledge support from the European Union through the COST Action MP0903.

References

- 1 C. S. Seney, B. M. Gutzman and R. H. Goddard, *The Journal of Physical Chemistry C*, 2009, **113**, 74–80.
- 2 Y. B. Zheng, L. Jensen, W. Yan, T. R. Walker, B. K. Juluri, L. Jensen and T. J. Huang, *The Journal of Physical Chemistry C*, 2009, **113**, 7019–7024.
- 3 W. A. Murray, B. Augu   and W. L. Barnes, *The Journal of Physical Chemistry C*, 2009, **113**, 5120–5125.
- 4 J. Z. Zhang, *The Journal of Physical Chemistry Letters*, 2010, **1**, 686–695.
- 5 H. Atwater and P. Albert, *Nature Materials*, 2010, **9**, 205–213.
- 6 S. E. Skrabalak, J. Chen, Y. Sun, X. Lu, L. Au, C. M. Cobley and Y. Xia, *Accounts of Chemical Research*, 2008, **41**, 1587–1595.
- 7 P. K. Jain, K. S. Lee, I. H. El-Sayed and M. A. El-Sayed, *The Journal of Physical Chemistry B*, 2006, **110**, 7238–7248.
- 8 R. Weissleder, *NATURE BIOTECHNOLOGY*, 2001, **19**, 316–317.
- 9 K. A. Schenkman, *Critical Care Science*, 2003, **30**, 267.
- 10 R. Bardhan, N. K. Grady, T. Ali and N. J. Halas, *ACS Nano*, 2010, **4**, 6169–6179.
- 11 O. Pe  a, U. Pal, L. Rodr  guez-Fern  ndez and A. Crespo-Sosa, *J. Opt. Soc. Am. B*, 2008, **25**, 1371–1379.
- 12 X.-B. Xu, Z. Yi, X.-B. Li, Y.-Y. Wang, X. Geng, J.-S. Luo, B.-C. Luo, Y.-G. Yi and Y.-J. Tang, *The Journal of Physical Chemistry C*, 2012, **116**, 24046–24053.
- 13 E. Cottancin, G. Celep, J. Lerm  , M. Pellarin, J. Huntzinger, J. Vialle and M. Broyer, *Theoretical Chemistry Accounts: Theory, Computation, and Modeling (Theoretica Chimica Acta)*, 2006, **116**, 514.
- 14 H.-Ch. Weissker, H. B. Escobar, V. D. Thanthirige, K. Kwak, D. Lee, G. Ramakrishna, R.L. Whetten, and X. L  pez-Lozano, *Nature Communications*, DOI: 10.1038/ncomms4785, 2014.
- 15 H.-Ch. Weissker and C. Mottet, *Phys. Rev. B*, 2011, **84**, 165443.
- 16 X. L  pez-Lozano, C. Mottet and H.-Ch. Weissker, *The Journal of Physical Chemistry C*, 2013, **117**, 3062–3068.
- 17 W. Ekardt, *Phys. Rev. B*, 1985, **31**, 6360–6370.
- 18 C. M. Aikens, S. Li and G. C. Schatz, *The Journal of Physical Chemistry C*, 2008, **112**, 11272.
- 19 G.-T. Bae and C. M. Aikens, *The Journal of Physical Chemistry C*, 2012, **116**, 10356–10367.
- 20 R. W. Burgess and V. J. Keast, *The Journal of Physical Chemistry C*, 2014, **118**, 3194–3201.
- 21 E. B. Guidez and C. M. Aikens, *Nanoscale*, 2012, **4**, 4190–4198.
- 22 E. B. Guidez and C. M. Aikens, *The Journal of Physical Chemistry C*, 2013, **117**, 12325–12336.
- 23 X. L  pez-Lozano, H. Barron, C. Mottet and H.-Ch. Weissker, *Phys. Chem. Chem. Phys.*, 2014, **16**, 1820–1823.
- 24 C. J. Heard and R. L. Johnston, *Phys. Chem. Chem. Phys.*, 2014, –.
- 25 N. Durante, A. Fortunelli, M. Broyer and M. Stener, *J. Phys. Chem. C*, 2011, **115**, 6277.
- 26 G. Barcaro, M. Broyer, N. Durante, A. Fortunelli and M. Stener, *The Journal of Physical Chemistry C*, 2011, **115**, 24085–24091.
- 27 M. Harb, F. Rabilloud and D. Simon, *Phys. Chem. Chem. Phys.*, 2010, **12**, 4246–4254.
- 28 R. W. Burgess and V. J. Keast, *The Journal of Physical Chemistry C*, 2011, **115**, 21016–21021.
- 29 G. Barcaro, L. Sementa, A. Fortunelli and M. Stener, *Nanoscale*, 2014, –.
- 30 O. L  pez-Acevedo, H. Tsunoyama, T. Tsukuda, H. H.

- and C. M. Aikens, *Journal of the American Chemical Society*, 2010, **132**, 8210–8218.
- 31 S. Malola, L. Lehtovaara, J. Enkovaara and H. Häkkinen, *ACS Nano*, 2013, **7**, 10263–10270.
- 32 F. Rabilloud, *The Journal of Physical Chemistry A*, 2013, **117**, 4267–4278.
- 33 M. E. Casida, *Recent Advances in Density Functional Methods, Part I*, 1995, p. 155.
- 34 M. E. Casida, *Recent Developments and Applications of Modern Density Functional Theory*, 1996, p. 391.
- 35 K. Yabana and G. F. Bertsch, *Phys. Rev. B*, 1996, **54**, 4484–4487.
- 36 S. Fedrigo, W. Harbich and J. Buttet, *Phys. Rev. B*, 1993, **47**, 10706–10715.
- 37 M. M. Alvarez, J. T. Khoury, T. G. Schaaff, M. Shafiqullin, I. Vezmar and R. L. Whetten, *J. Phys. Chem. B*, 1997, **101**, 3706.
- 38 B. Prével, J. Lermé, M. Gaudry, E. Cottancin, M. Pel-larin, M. Treilleux, P. Mélinon, A. Perez, J. L. Vialle and M. Broyer, *Scripta Materialia*, 2001, **44**, 1235.
- 39 Z. Y. Li, J. P. Wilcoxon, F. Yin, Y. Chen, R. E. Palmer and R. L. Johnston, *Faraday Discuss.*, 2008, **138**, 363–373.
- 40 S. Gilb, K. Hartl, A. Kartouzian, J. Peter, U. Heiz, H.-G. Boyen and P. Ziemann, *Eur. Phys. J. D*, 2007, **45**, 501–506.
- 41 M. Zhu, C. M. Aikens, F. J. Hollander, G. C. Schatz and R. Jin, *Journal of the American Chemical Society*, 2008, **130**, 5883–5885.
- 42 H. Qian, Y. Zhu and R. Jin, *Proceedings of the National Academy of Sciences*, 2012.
- 43 A. C. Dharmaratne and A. Dass, *Chem. Commun.*, 2014, **50**, 1722–1724.
- 44 K. J. Taylor, C. L. Pettiette-Hall, O. Cheshnovsky and R. E. Smalley, *The Journal of Chemical Physics*, 1992, **96**, 3319–3329.
- 45 H. Wang, F. Tam, N. K. Grady and N. J. Halas, *The Journal of Physical Chemistry B*, 2005, **109**, 18218–18222.
- 46 H. Hakkinen, *Chem. Soc. Rev.*, 2008, **37**, 1847–1859.
- 47 A. J. Karttunen, M. Linnolahti, T. A. Pakkanen and P. Pyykko, *Chem. Commun.*, 2008, 465–467.
- 48 F. Baletto and R. Ferrando, *Rev. Mod. Phys.*, 2005, **77**, 371–423.
- 49 G. Kresse and J. Furthmüller, *Comput. Mat. Sci.*, 1996, **6**, 15.
- 50 G. Kresse and D. Joubert, *Phys. Rev. B*, 1999, **59**, 1758.
- 51 J. P. Perdew, J. A. Chevary, S. H. Vosko, K. A. Jackson, M. R. Pederson, D. J. Singh and C. Fiolhais, *Phys. Rev. B*, 1992, **46**, 6671–6687.
- 52 M. A. L. Marques, A. Castro, G. F. Bertsch and A. Rubio, *Comp. Phys. Comm.*, 2003, **151**, 60.
- 53 A. Castro, M. A. L. Marques, H. Appel, M. Oliveira, C. Rozzi, X. Andrade, F. Lorenzen, E. K. U. Gross and A. Rubio, *Phys. Stat. Sol. (b)*, 2006, **243**, 2465.
- 54 A. Castro, M. A. L. Marques, A. H. Romero, M. J. T. Oliveira and A. Rubio, *The Journal of Chemical Physics*, 2008, **129**, 144100.
- 55 M. Stener, A. Nardelli and G. Fronzoni, *The Journal of Chemical Physics*, 2008, **128**, –.
- 56 H.-C. Weissker, N. Ning, F. Bechstedt and H. Vach, *Phys. Rev. B*, 2011, **83**, 125413.